ELSEVIER
Cold Regions Science and Technology 28 (1998) 29–44
cold regions science and technology

Numerical simulations of frazil ice dynamics in the upper layers of the ocean

Urban Svensson [a,1], Anders Omstedt [b,*]

[a] *Computer-aided Fluid Engineering, S-602 10 Norrköping, Sweden*
[b] *SMHI, S-601 76 Norrköping, Sweden*

Received 1 October 1997; accepted 12 May 1998

Abstract

The frazil ice dynamics in a turbulent Ekman layer have been investigated using a mathematical model. The model is based on the conservation equations for mean momentum, energy and salinity, and employs a two-equation turbulence model for the determination of turbulent diffusion coefficients. A crystal number continuity equation is used for the prediction of the frazil ice dynamics. This equation considers several processes of importance, as for example turbulent diffusion, gravitational up-drift, flocculation/break-up and growth. The results focus on the frazil ice characteristics in the upper layers of the ocean, like suspended ice volume, ice crystals per m^3, vertical distributions, etc. From the idealized calculations, it is indicated that a large number of ice crystals can be mixed into the ocean during freezing. However, the amount of ice in suspension, measured as vertically integrated ice thickness, adds only a minor part to the total surface ice budget. Small crystals are mixed deep in the ocean while the large ones are found only in the top of the mixed layer. Knowledge about the vertical distribution of ice crystals of different sizes, which is calculated from the model, should be of importance when analysing processes as formation of ice covers in the ocean and ice–sediment or ice–algae interaction.

Keywords: Frazil ice; Ekman layer; Turbulence

1. Introduction

Almost all ice models applied in the polar and sub-polar seas are based upon models derivated from the one-dimensional heat conduction equation (e.g., Stefan, 1891; Maykut and Untersteiner, 1971; Hibler, 1979; Leppäranta, 1983, 1993; Maykut, 1986). They assume some initial ice thickness, from which the ice is assumed to grow, and sometimes simplify the problem by introducing the so-called freezing degree-day method or assuming a linear temperature change in the ice, and the ice growth becomes propotional to the square root of time. The physical processes in mind using the above method, are related to columnar ice growth. In the ocean, the initial ice formation is, however, often related to frazil ice formation, in which all heat losses from the open water is transformed into suspended ice crystals and the ice growth becomes linear with time. Frazil ice

* Corresponding author. Tel.: +46-11-495-8284; Fax: +46-11-495-8001; E-mail: anders.omstedt@smhi.se
[1] Tel.: +46-11-13-00-12; Fax: +46-11-13-00-12; E-mail: us@cfe.se.

0165-232X/98/$ - see front matter
PII: S0165-232X(98)00011-1

formation is associated with large heat fluxes to the atmosphere, large ice production and large amount of salt rejected from the ice crystals into the ocean.

Intensive studies of the cold seas, during the last decades, have demonstrated the importance of frazil ice. The major sea ice forming process in the Wedell Sea, Antarctica, is due to frazil ice that is transformed to pancake ice at the surface due to wave–ice interaction (Wadhams et al., 1987; Lange, 1990). Ice core measurements from the Wedell Sea illustrate that frazil ice contribute with as much as 50% of the ice mass (Gow et al., 1982).

In the Arctic new ice often forms on the shallow shelves through frazil ice formation (Pfirman et al., 1990). In these shallow areas large amounts of sediments can be incorporated and mixed in the ice through the frazil ice formation and escape from the shelf region through advection out into the Beufort Sea or into the Transport drift stream out through the Fram Strait.

In polynyas, leads and at ice edges frazil ice is the main ice process (e.g., Martin, 1981; Pease, 1987; Smith et al., 1990; Ushio and Wakatsuchi, 1993; Wadhams et al., 1996). For the ventilation of intermediate and deep water masses in the Arctic, frazil ice formation on the shelves is believed to play an important role in forming dense water masses (Aagard et al., 1981; Martin and Cavalieri, 1989). As the small frazil ice crystals become suspended in the upper layers of the ocean, they can actively interact both with the mixed layer dynamics as well as sedimentary particles (Reimnitz and Kempema, 1987; Kempema et al., 1988; Pfirman et al., 1990; Nurnberg et al., 1994).

The frazil ice crystals also strongly interact with the biological communities in the upper layers of the ocean (Ackley and Sullivan, 1994). The structure of an ice cover formed through frazil ice is therefore different compared to that of columnar ice, with sediment particles and biological material vertically mixed within the whole ice column. Modelling of frazil ice beneath ice shelves has been done by, for e.g., Bombosch and Jenkins (1995) and Jenkins and Bombosch (1995), but this will not be further dealt with in the present work, instead we only consider frazil ice formation in the upper layers of the ocean.

As the physics of frazil ice differs from columnar ice, new efforts are needed to properly simulate or parameterize the ice–ocean interaction. Some field and laboratory experiments on frazil ice formation have been conducted, but rather few models are available today. Modelling efforts were made by Bauer and Martin (1983), when they considered the ice formation in leads, while Pease (1987) treated wind driven polynyas. Martin and Cavalieri (1989) further estimated the role of the Siberian Shelf polynyas in generating dense water through frazil ice formation. In these studies, the ice formation was assumed to be due to frazil ice, however, no models or ideas about the frazil ice dynamics were introduced instead bulk heat balance arguments were applied. In a series of papers (Omstedt and Svensson, 1984; Omstedt, 1985a,b), a frazil ice model for the upper layers of the ocean was developed. The main achievements were that the ice formation could be treated as a boundary layer problem and that no assumption was needed when ice was forming. Instead the initial ice formation and growth were treated by the model through physically sound assumptions. In the model, the frazil ice growth was assumed to be due to multiplication, and a constant crystal size was assumed. In a later study, Svensson and Omstedt (1994) presented a model of frazil ice dynamics, where the crystal number continuity equation was solved for a well mixed jar.

The present work will extend the frazil ice model by Svensson and Omstedt (1994) to the upper layers of the ocean and examine the dynamics of frazil ice formation in an Ekman boundary layer. The purpose is to describe and discuss processes involved in the generation of ice due to surface cooling. This involves transport processes in the vertical direction, due to turbulent diffusion and gravitational rise, as well as dynamical processes, like growth and flocculation, in radial space.

The outline of the paper is as follows. In Section 2, a general description of frazil ice is given. Then in Section 3, the mathematical formulation is outlined. Section 4 gives the results and finally, some conclusions are given in Section 5.

2. General description

A thorough review of the physics of frazil ice has recently been given by Daly (1994); there is thus no need to review the subject in the present paper. The basic features of the situation studied will, however, be briefly introduced, see Fig. 1.

The problem will be discussed in boundary layer terms, and the hydrodynamical scene is thus a turbulent Ekman layer. In the present context, the main interest in the hydrodynamics is that it provides a turbulent diffusion coefficient. If heat is lost at the surface, the turbulent diffusion coefficient will have a strong influence on the resulting temperature distribution. During the formation of frazil ice salt is rejected into the water phase. Also the resulting salinity profile is strongly governed by the magnitude and distribution of the turbulent diffusion coefficient. There is a coupling back to the turbulence field from the distributions of temperature, salinity and frazil ice, as these modifies the mixture density distribution, which, in turn, affects the turbulence level.

The physical processes believed to be the most important ones in the frazil ice dynamics are listed in Fig. 1. Seeding is the term used for the mass exchange at the ocean surface caused by aerosols. It is known, from laboratory studies, that seeding is primarily important for the initialisation of frazil ice (heterogeneous nucleation). When the frazil ice regime is established, small ice fragments are shed from large ice crystals (secondary nucleation or collision breeding). The intensity of the breeding is a function of the turbulence intensity, which gives a further link to the hydrodynamics. The small ice fragments then act as nucleus for growth. Regarding the growth of ice crystals, we will assume that crystals are disc-shaped and grow only at the edges. The crystal size distribution is also influenced by flocculation and break-up. In the present formulation, it will be assumed that the net effect is a transport to larger aggregates. Due to gravity some

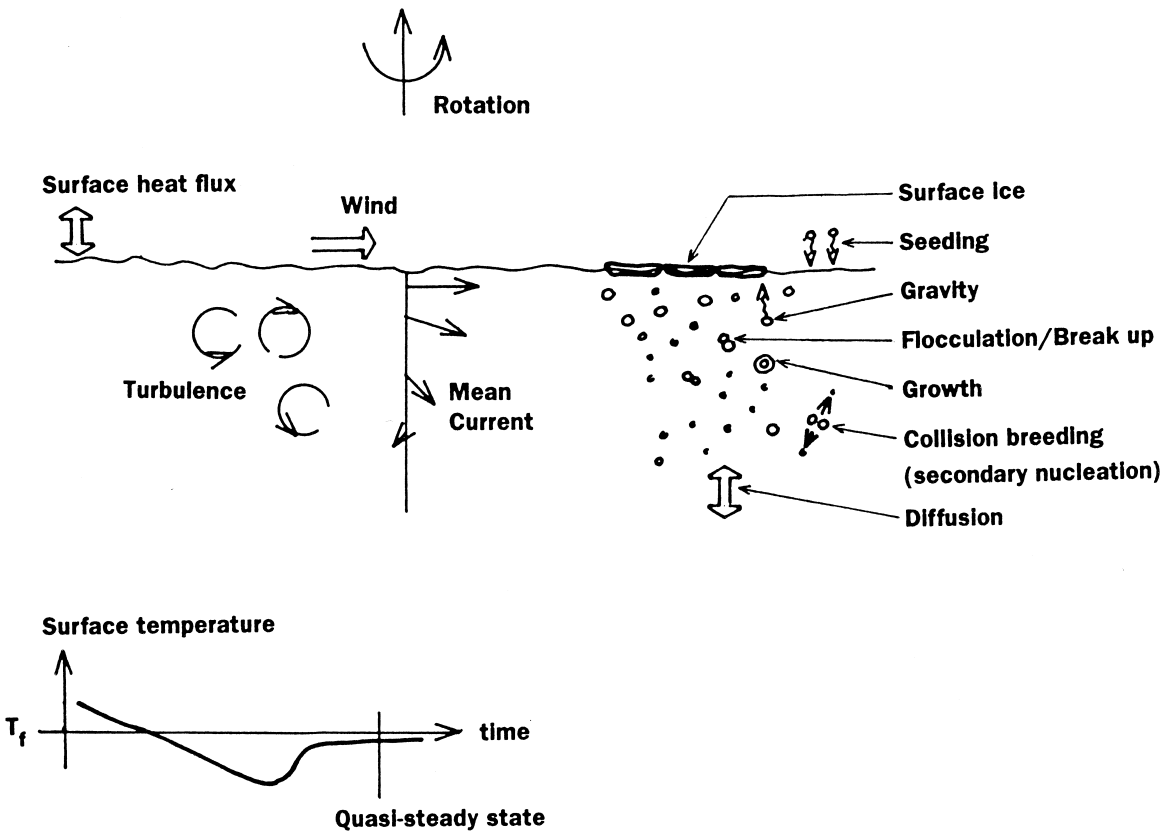

Fig. 1. Schematic outline of the problem studied.

of the suspended ice will reach the surface and form surface ice, frazil slush which may form pancake ice. This is the final process in the link from surface heat loss to surface ice.

The transient nature of the problem is also shown in Fig. 1. Assuming that the wind stress and the surface cooling are constant in time, the surface water temperature will develop as outlined. After the temperature for freezing, T_f, is reached, supercooling starts. Soon after that time, ice formation starts, but initially at a rather low rate because of the small ice area exposed to the supercooled water. The supercooling will thus increase until the time of maximum supercooling; after that, freezing releases more heat than is lost at the surface. Eventually a quasi-stationary situation is reached, when the product of exposed ice area and supercooling is proportional to the surface cooling. In this paper we will focus interest on this quasi-steady state, as it is in this stage that most frazil ice is produced.

The situation outlined in Fig. 1 assumes that horizontally homogeneous conditions prevail. When a certain amount of surface ice has formed, this ice will cause a non-uniform surface wind stress and heat flux. The model is thus relevant only for a limited time. However, the surface ice may be transported away by the wind and the water surface is kept free, as in the case of polynyas. The model is then valid as long as the water surface is free. In this paper, we will not further concern ourselves with the practical application of the model, but concentrate on the frazil ice dynamics in the quasi-steady state as marked in Fig. 1.

3. Mathematical formulation

3.1. Basic assumption

The present model can, as mentioned above, be considered as a combination of the models of Omstedt and Svensson (1984) and Svensson and Omstedt (1994). In fact, we will keep basic assumptions, material properties, numerical coefficients, etc. exactly as given in these two papers. This has the advantage that the basic verification studies presented by Svensson and Omstedt (1994) are valid also for the present formulation. We may also refer to these two papers for a thorough discussion of basic assumptions and details about the model formulation.

3.2. Mean flow equations

Within the assumptions made, the mean flow equations take the following form:

$$\frac{\partial S}{\partial t} = \frac{\partial}{\partial z}\left(\frac{\upsilon_T}{\sigma_S}\frac{\partial S}{\partial z}\right) + G_s \tag{1}$$

$$\frac{\partial T}{\partial t} = \frac{\partial}{\partial z}\left(\frac{\upsilon_T}{\sigma_T}\frac{\partial T}{\partial z}\right) + G_T \tag{2}$$

$$\frac{\partial U}{\partial t} = \frac{\partial}{\partial z}\left(\upsilon_T\frac{\partial U}{\partial z}\right) + fV \tag{3}$$

$$\frac{\partial V}{\partial t} = \frac{\partial}{\partial z}\left(\upsilon_T\frac{\partial V}{\partial z}\right) - fU \tag{4}$$

where z is the vertical space coordinate positive upwards, t the time coordinate, f the Coriolis' parameter, U and V are mean velocities in horizontal directions, S is the mean salinity, and T the mean temperature. The kinematic eddy viscosity is denoted by υ_T, σ_s and σ_T are Prandtl/Schmidt numbers for salinity and temperature, respectively. Source/sink terms in the equations for salinity and temperature are denoted by G_S and G_T, respectively.

The source terms, which are due to the freezing and melting of ice, can be derived by considering a unit volume of a mixture of water and ice particles. The heat flux per unit area of ice, q, between the water and ice, can be expressed as

$$q = \mathrm{Nu}\, k_w (T_i - T)(d^{-1}) \ (\mathrm{W\,m^{-2}}) \tag{5}$$

where Nu is the Nusselt number, k_w is the thermal conductivity for water, d a characteristic length (here taken as the disc thickness) and T_i is the ice surface temperature, taken as the freezing temperature in the following calculations. Considering the unit volume with frazil ice with a total area, A, exposed to freezing or melting, it can be shown (Omstedt, 1985b) that the term in the temperature equation takes the form

$$G_T = qA(\rho_w c_p)^{-1} \ (^\circ\mathrm{C\,s^{-1}}) \tag{6}$$

where ρ_w is the density of water and c_p the specific heat of water. The heat flux, it is assumed, will be directly related to melting or freezing.

By assuming that the ice has zero salinity, an expression for the source/sink term in the equation for the salinity of the water may be formulated as

$$G_S = SqA(L\rho_w)^{-1}\ (\mathrm{s}^{-1}) \tag{7}$$

where L is the latent heat of ice.

3.3. Turbulence model

The turbulence model used in this paper is based on turbulent exchange coefficients calculated from a kinetic energy-dissipation model of turbulence. The equations can be derived in exact form from the Navier–Stokes equations and are thereafter 'modelled' to the following form:

$$\frac{\partial k}{\partial t} = \frac{\partial}{\partial z}\left(\frac{\upsilon_T}{\sigma_k}\frac{\partial k}{\partial z}\right) + P_s + P_b - \varepsilon \tag{8}$$

$$\frac{\partial \varepsilon}{\partial t} = \frac{\partial}{\partial z}\left(\frac{\upsilon_T}{\sigma_\varepsilon}\frac{\partial \varepsilon}{\partial z}\right) + \frac{\varepsilon}{k}(C_{1\varepsilon}P_s + C_{3\varepsilon}P_b - c_{2\varepsilon}\varepsilon) \tag{9}$$

$$P_s = \left(\left(\frac{\partial U}{\partial z}\right)^2 + \left(\frac{\partial V}{\partial z}\right)^2\right) \tag{10}$$

$$P_b = \upsilon_T g\left(-2\alpha\frac{(T-T_M)}{\sigma_T}\frac{\partial T}{\partial z} + \frac{\beta}{\sigma_s}\frac{\partial S}{\partial z} + \frac{(\rho_i - \rho_o)}{\sigma_c\,\rho_o}\frac{\partial C}{\partial z}\right) \tag{11}$$

$$\upsilon_T = C_\mu\frac{k^2}{\varepsilon} \tag{12}$$

where k is the turbulent kinetic energy, ε its dissipation rate, P_s production due to shear and P_b is production/destruction due to buoyancy, C the volume fraction of ice and σ_c, the Schmidt number for ice crystals. The kinematic eddy viscosity is denoted υ_T. For a general description of this turbulence model the reader is referred to Rodi (1980, 1987).

3.4. Equation of state

An underlying assumption of the P_b term is that the ice and the water can be regarded as a mixture when considering buoyancy effects in the turbulence model. The mixture density ρ_m can be calculated from

$$\rho_m = \rho_w + C(\rho_i - \rho_w) \tag{13}$$

where ρ_i is the ice density.

The density of water, ρ_w, in this temperature interval is an almost quadratic function of temperature and is also linearly dependent on salinity. An approximative form, also used by Omstedt et al. (1983), reads

$$\rho_w = \rho_o\left(1 - \alpha(T-T_M)^2 + \beta S\right) \tag{14}$$

where α and β are constants, T_M is temperature of maximum density, and ρ_o a reference density. The temperature of maximum density, as well as the freezing temperature, is a function of salinity and pressure. In the present study both of these temperatures will, however, be set to constants adequate for sea surface pressure and a salinity of 5‰, see Table 1.

Table 1
Model constants

	Constants	Value	Unit
C_μ	constant in the turbulence model	0.09	–
$C_{1\varepsilon}$	constant in the turbulence model	1.44	–
$C_{2\varepsilon}$	constant in the turbulence model	1.92	–
$C_{3\varepsilon}$	constant in the turbulence model	0.8	–
σ_k	Prandtl/Schmidt number	1.4	–
σ_ε	Prandtl/Schmidt number	1.3	
σ_c	Prandtl/Schmidt number	1.0	
σ_T	Prandtl/Schmidt number	1.0	
σ_s	Prandtl/Schmidt number	1.0	
σ_n	Prandtl/Schmidt number	1.0	
α	constant in the equation of state	5.6×10^{-6}	$°C^{-2}$
β	constant in the equation of state	8.0×10^{-4}	‰$^{-1}$
ρ_0	reference density	1.0×10^{3}	kg m^{-3}
T_M	temperature of maximum density	2.9	°C
T_f	freezing temperature	-0.3	°C
f	Coriolis' parameter	1.3×10^{-4}	s^{-1}
Nu	Nusselt number	1.0	
d	ice disc thickness	10^{-5}	m
k_w	thermal conductivity	0.564	W (m °C)$^{-1}$
L	latent heat of pure ice	3.34×10^{5}	J kg^{-1}
ρ_i	density of ice	9.2×10^{2}	kg m^{-3}
c_p	specific heat of water	4.217×10^{3}	J (kg °C)$^{-1}$

3.5. Crystal number continuity equation

Assume that the frazil ice particles can be classified into N discrete radius intervals, within which all

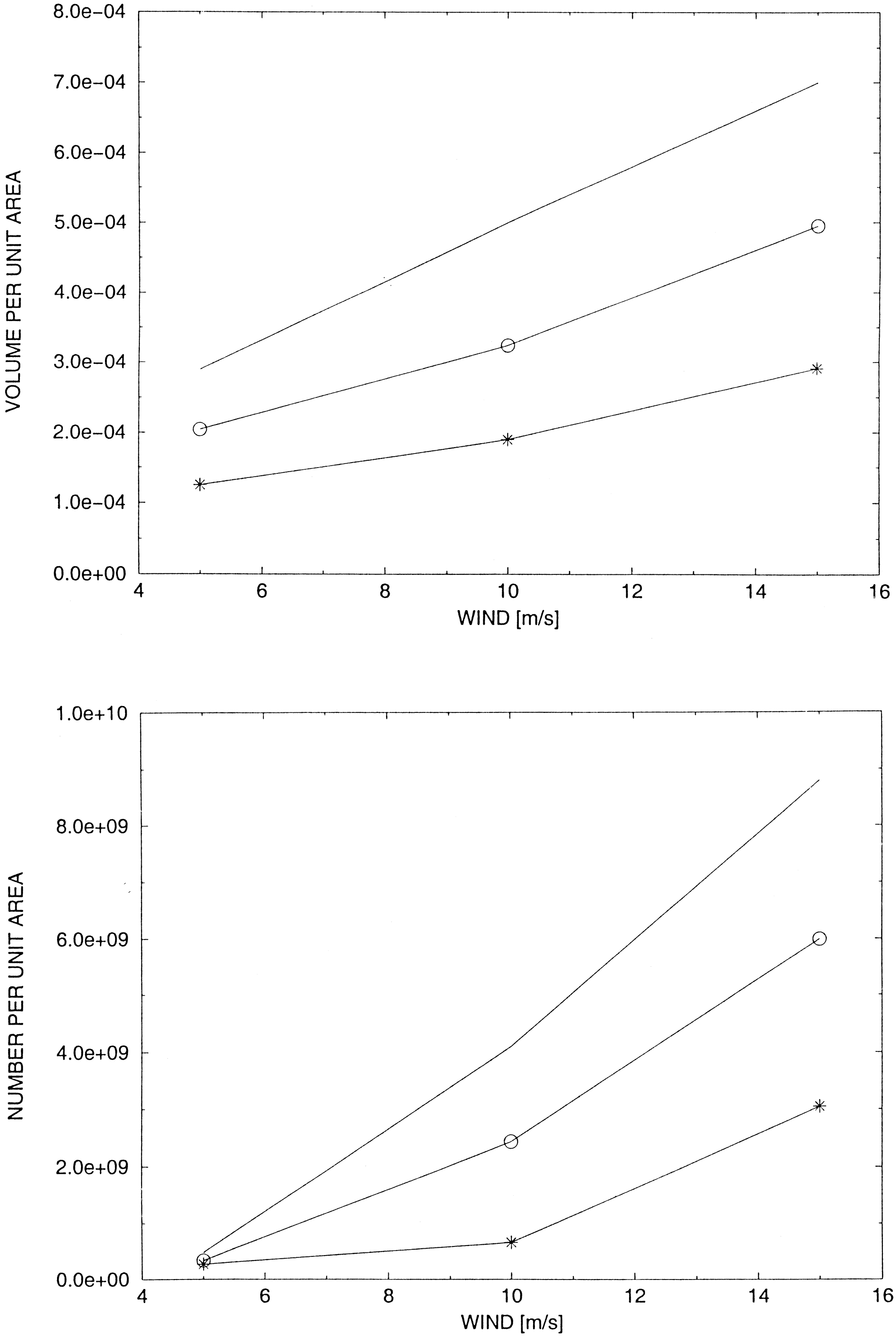

Fig. 2. The depth-integrated volume (top) of ice and number of crystals as a function of wind speed and surface cooling. (————) 300 W/m^2; (——○——) 200 W/m^2; (——∗——) 100 W/m^2.

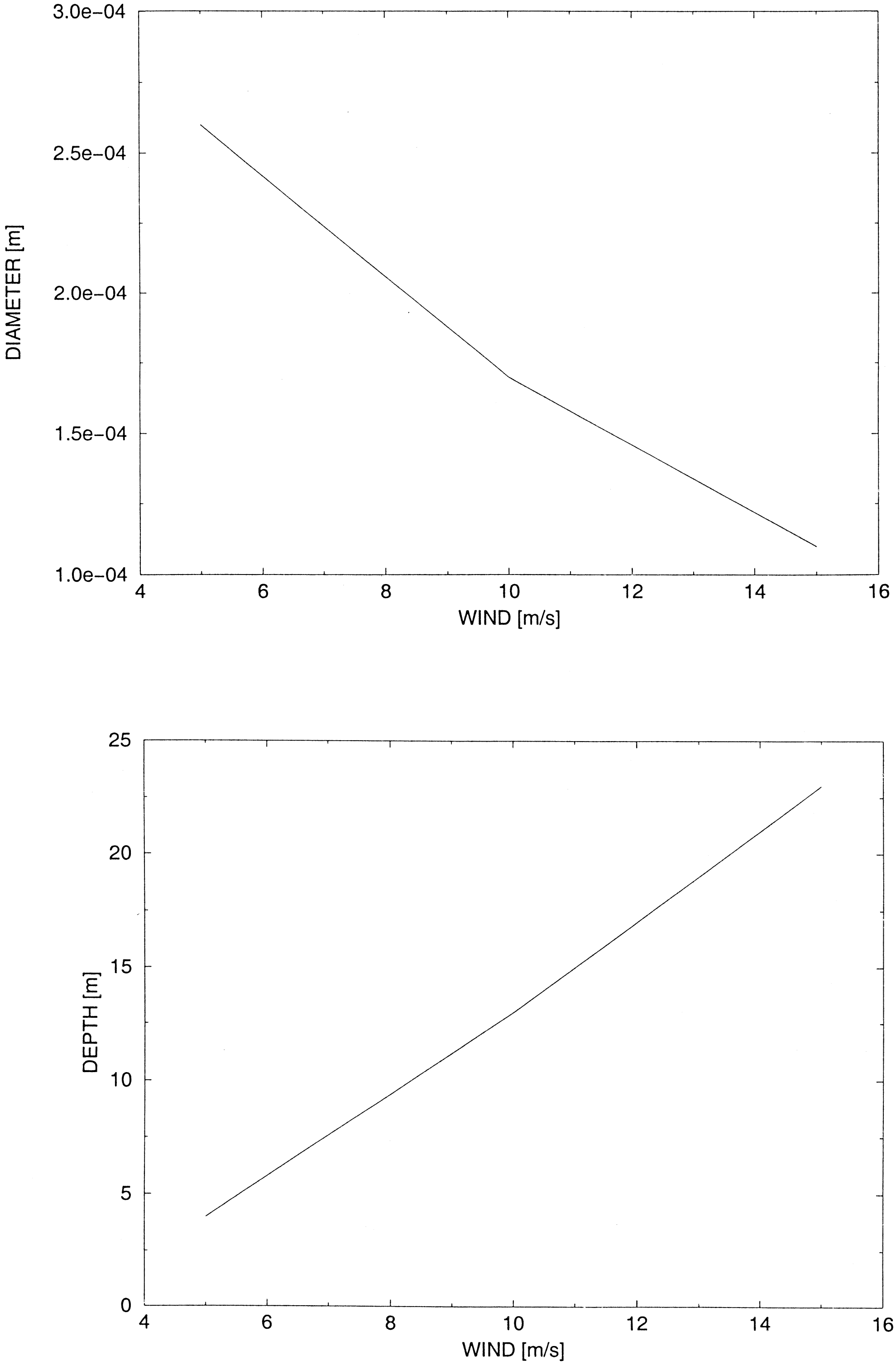

Fig. 3. Depth-integrated properties. Mean diameter (top) and penetration depth (90% of volume). Surface cooling: 200 W/m^2.

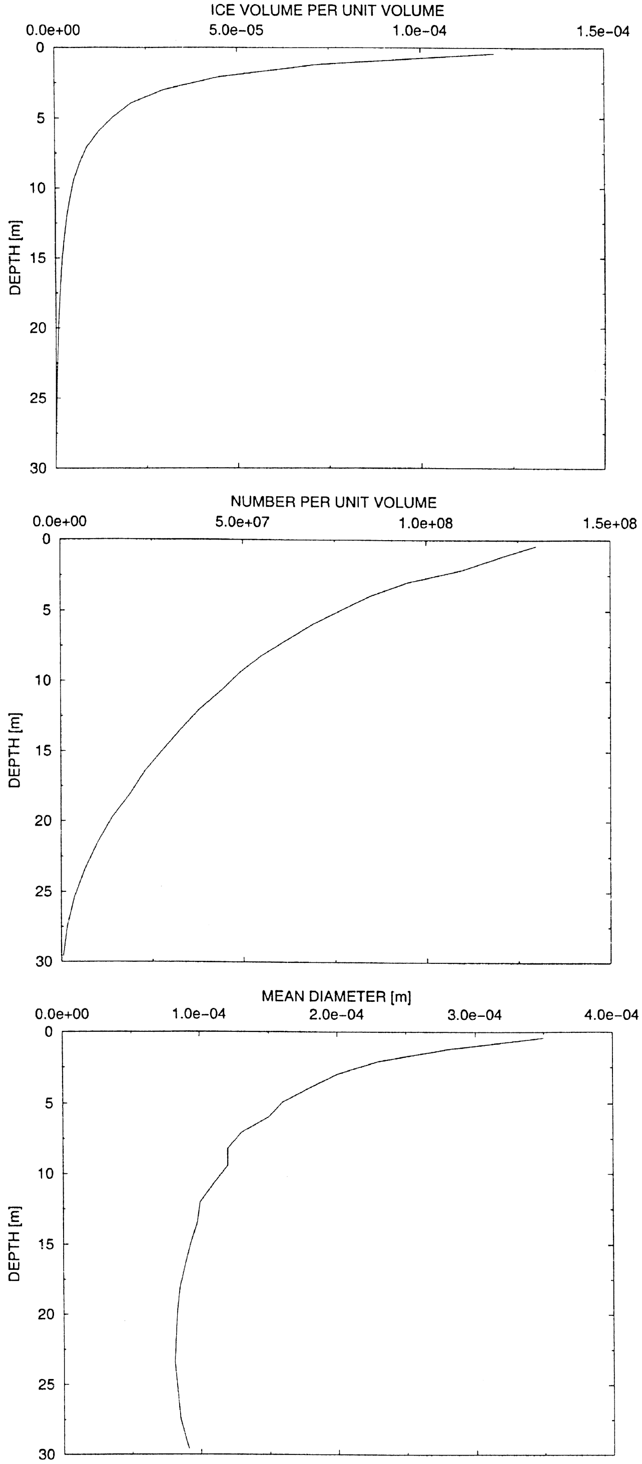

Fig. 4. Vertical distributions. Frazil ice volume (top), number of crystals (middle) and mean diameter. Windspeed: 10 m/s. Surface cooling: 200 W/m^2.

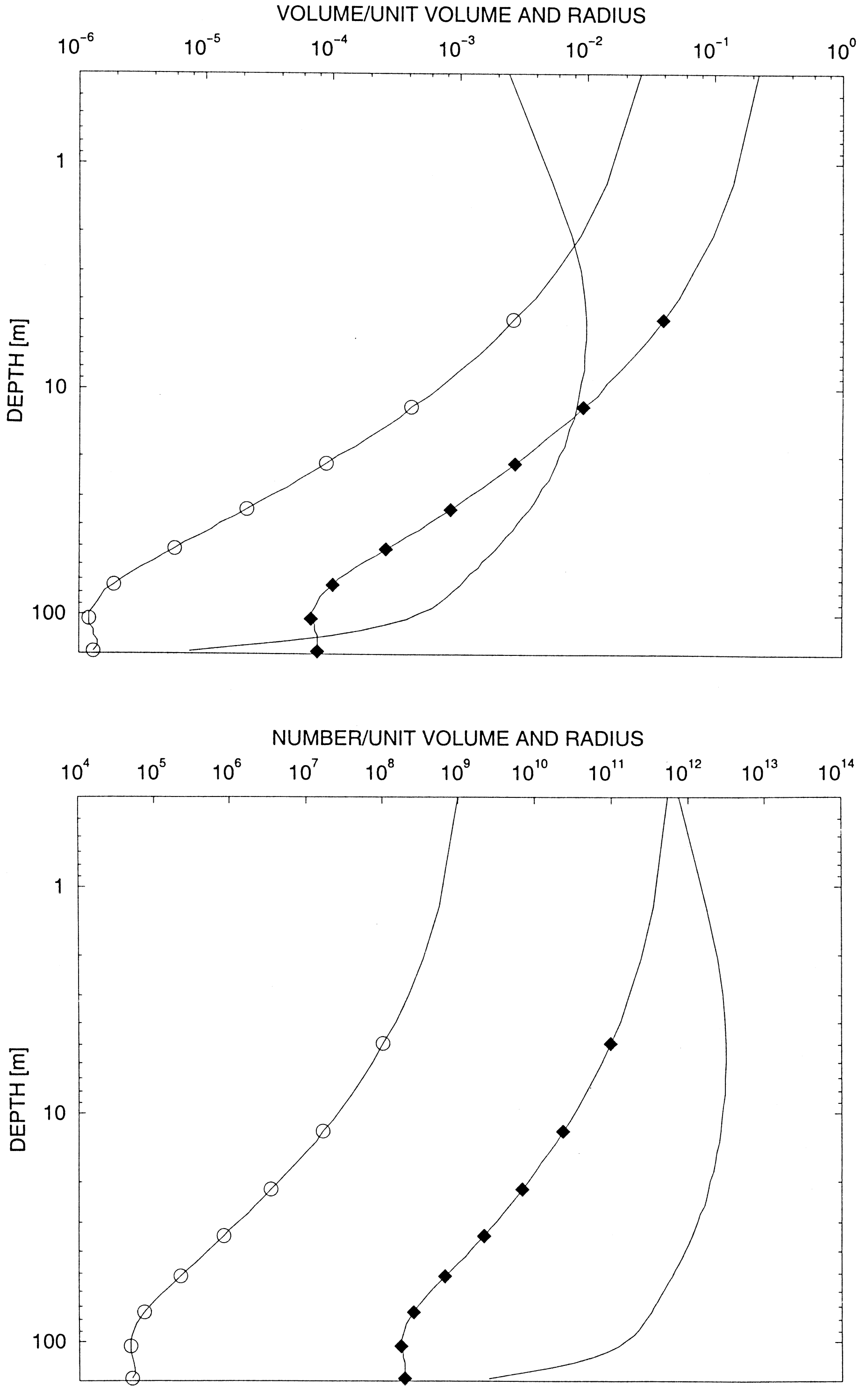

Fig. 5. Volume (top) and number of three crystal sizes as a function of depth. (———) $r = 10^{-5}$; (——♦——) $r = 10^{-4}$; (——○——) $r = 10^{-3}$ W/m^2. Windspeed: 10 m/s. Surface cooling: 200 W/m^2.

particles are assumed to be of equal radius. The following equation can be then formulated for the number of particles, n_i, in each group:

$$\underbrace{\frac{\partial n_i}{\partial t}}_{\text{Change in number}} = \underbrace{\frac{\partial}{\partial z}\left(\frac{\nu_{\mathrm{T}}}{\sigma_{\mathrm{n}}}\frac{\partial n_i}{\partial z}\right)}_{\text{Diffusion}} \underbrace{- W_i \frac{\partial n_i}{\partial z}}_{\text{Gravity}}$$

$$\underbrace{+ \underset{(i=1)}{\sum_{j=2}^{N} \alpha_j n_i} - \underset{(2 \le i \le N)}{\alpha_i n_i}}_{\text{Secondary nucleation}}$$

$$\underbrace{- \underset{(1 \le i \le N-1)}{\beta_i n_i} + \underset{(2 \le i \le N)}{\delta \beta_{i-1} n_{i-1}}}_{\text{Floccul./break-up}}$$

$$\underbrace{- \underset{(1 \le i \le N-1)}{\Gamma_i n_i} + \underset{(2 \le i \le N)}{\Gamma_{i-1} n_{i-1}}}_{\text{Crystal growth}} \qquad (15)$$

where α_j, β_i, Γ_i are coefficients [s^{-1}] giving the strength of the process considered. The gravitational rise velocity is denoted W_i and σ_{n} is a Prandtl/Schmidt number. The factor δ is the ratio between volumes of particles of two neighbouring radius intervals. Eq. (15) gives the evolution of the particle size distribution from an initial stage, given the values of the coefficients. The left hand side of Eq. (15) gives the change in number of crystals in radius interval i. This change is due to the processes on the right hand side of the equation. Turbulent diffusion will redistribute the particles, while gravity will always generate an upward drift. The term secondary nucleation gives a source for the smallest radius interval, $i = 1$, and a corresponding sink for other intervals. The two terms in flocculation/break-up and crystal growth are due to the discretization concept used; crystals are entering from a smaller radius and leave the present interval to enter the next higher one.

Expressions for the coefficients in Eq. (15) and further background and details are given by Svensson and Omstedt (1994).

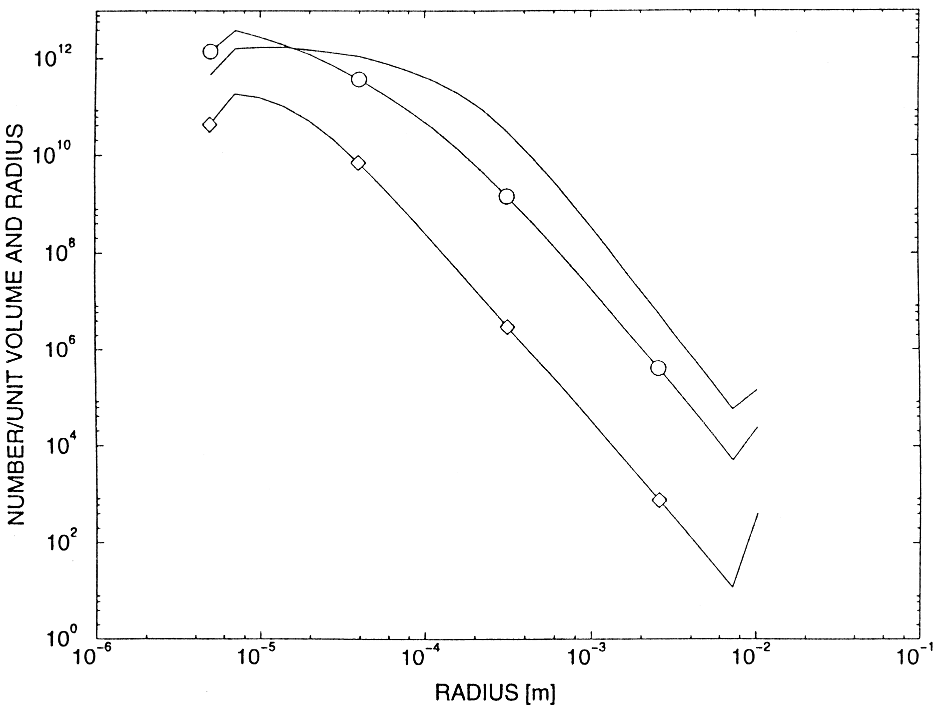

Fig. 6. Number of crystals at three selected depths, as a function of radius. (————) 1 m; (——○——) 10 m; (——◇——) 100 m depth. Windspeed: 10 m/s. Surface cooling: 200 W/m^2.

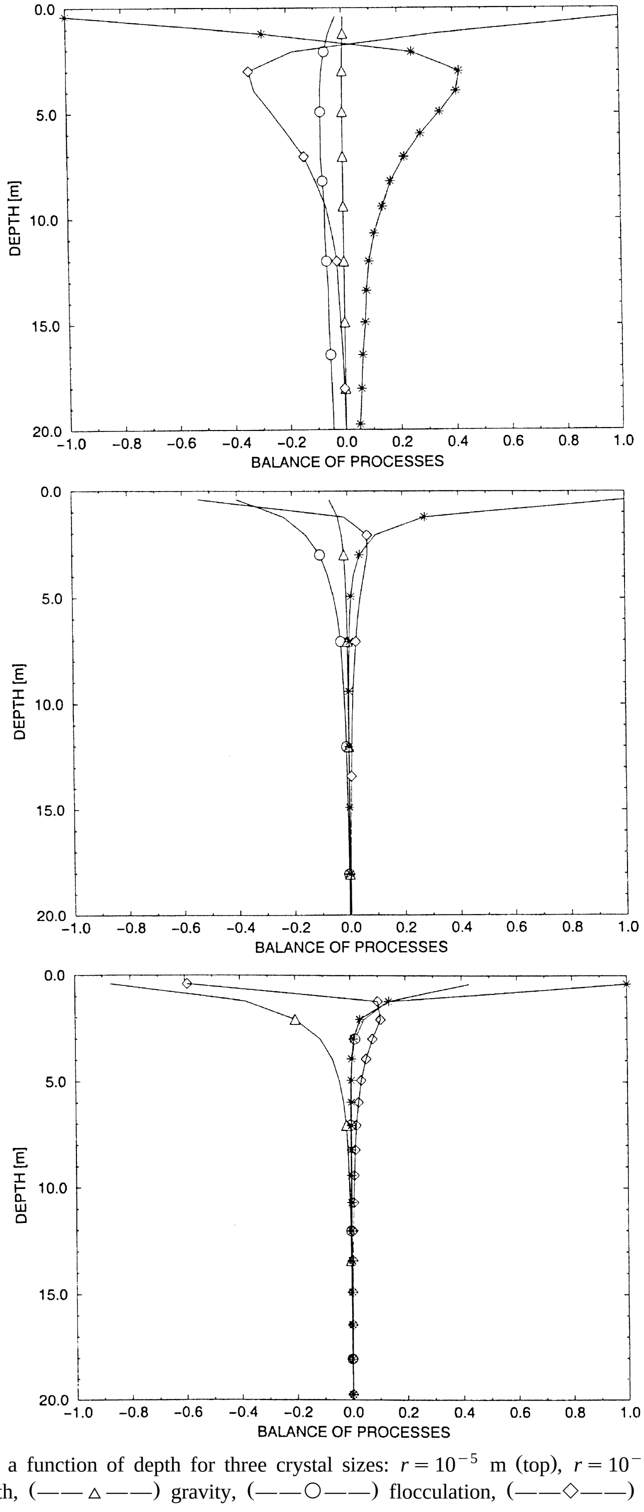

Fig. 7. Balance of processes as a function of depth for three crystal sizes: $r = 10^{-5}$ m (top), $r = 10^{-4}$ m (middle) and $r = 10^{-3}$ m. Processes: (——$*$——) growth, (——$\triangle$——) gravity, (——○——) flocculation, (——◇——) diffusion. Windspeed: 10 m/s. Surface cooling: 200 W/m^2.

3.6. Boundary and initial conditions

Surface boundary conditions for mean flow variables are specified according to:

$$\frac{\upsilon_\mathrm{T}}{\sigma_\mathrm{T}}\frac{\partial T}{\partial z}=F_\mathrm{N}(\rho_\mathrm{o}c_\mathrm{p})^{-1} \tag{16}$$

$$\frac{\upsilon_\mathrm{T}}{\sigma_\mathrm{s}}\frac{\partial S}{\partial z}=0 \tag{17}$$

$$\frac{\upsilon_\mathrm{T}}{\sigma_\mathrm{T}}\frac{\partial U}{\partial z}=\tau_x\rho_\mathrm{o}^{-1} \tag{18}$$

$$\frac{\upsilon_\mathrm{T}}{\sigma_\mathrm{T}}\frac{\partial V}{\partial z}=\tau_x\rho_\mathrm{o}^{-1} \tag{19}$$

where τ_x and τ_y are wind stresses and F_N is net heat flux. The zero flux condition for salinity is an approximation made in this analysis, as precipitation and evaporation rates generate a non zero flux. The results are not particularly sensitive to this approximation. The wind stress is calculated from the wind speed at 10 m, using a drag-coefficient of 1.3×10^{-3}. The turbulent kinetic energy k and its dissipation rate ε are related to the friction velocity at the surface. For details, see Rodi (1987).

For ice particles, the flux through the water surface (forming surface ice) is due to gravity. For particle size i the flux is $W_i n_i$. The exception is the smallest size ($i=1$) where a small downward flux (1000 particles s^{-1} m^{-2}) is prescribed. This seeding is important in the initial phase of the frazil build-up, but has no effect in the quasi-steady state studied here.

At the lower boundary a zero flux condition is used for all variables.

Initial conditions are given as zero velocity, -0.3°C temperature, 1000 ice particles in each radius interval and 5‰ salinity (a typical value for the northern extension of the Baltic Sea). The initial number of ice particles will not influence the results for the quasi-steady state.

3.7. Numerical solution

Eqs. (1)–(19) form a closed system and thus constitute the mathematical model. This set of equations, in their finite difference form, was integrated forward in time by using an implicit scheme and a standard tri-diagonal matrix algorithm (Svensson, 1986).

The numerical solutions were tested for and found to be grid- and time step-independent. This was achieved by a grid expanding from the surface with a total of 50 grid cells covering a depth of 150 m. The time step was chosen to 600 s for cooling down to the freezing temperature and to 1 s for further cooling.

For the frazil ice 23 radius intervals were used, covering a radius interval from $5.\times10^{-6}$ to $1.\times10^{-2}$ m.

4. Results and discussion

In this section, results from numerical simulations will be presented and discussed. First, depth integrated properties are presented, then distributions in the vertical and radial coordinate are shown. Finally, we study the balance of various processes in the crystal number equation.

4.1. Depth integrated properties

In Fig. 2, the depth integrated volume of ice and the number of crystals are shown. These parameters are given as function of wind and surface cooling rate. The depth-integrated volume $[\mathrm{m}^3/\mathrm{m}^2]$ can be interpreted as the thickness of an ice cover. We find from Fig. 2 that this ice-cover is less than a millimetre thick. The number of ice crystals is found to be of the order 10^9. The number of crystals suspended in the surface layer is thus very large, but still frazil ice in suspension represents only a small ice volume, almost negligible, compared to typical surface ice budget values.

Fig. 3 shows the typical penetration depth, determined as the depth holding 90% of the total volume,

Fig. 8. Balance of processes as a function of radius, at two selected depths, 1 m (top) and 10 m. Processes: (——∗——) growth, (——△——) gravity, (——○——) flocculation, (——◇——) diffusion. Windspeed: 10 m/s. Surface cooling: 200 W/m^2.

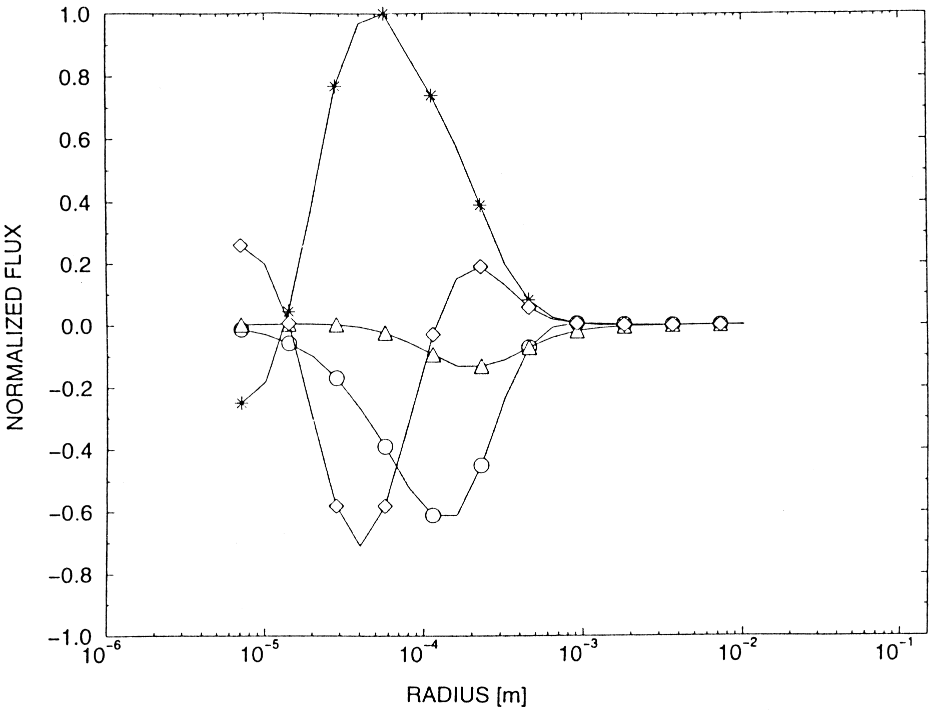
1.0
0.8
0.6
0.4
0.2
0.0
−0.2
−0.4
−0.6
−0.8
−1.0
NORMALIZED FLUX
10^{-6}
10^{-5}
10^{-4}
10^{-3}
10^{-2}
10^{-1}
RADIUS [m]

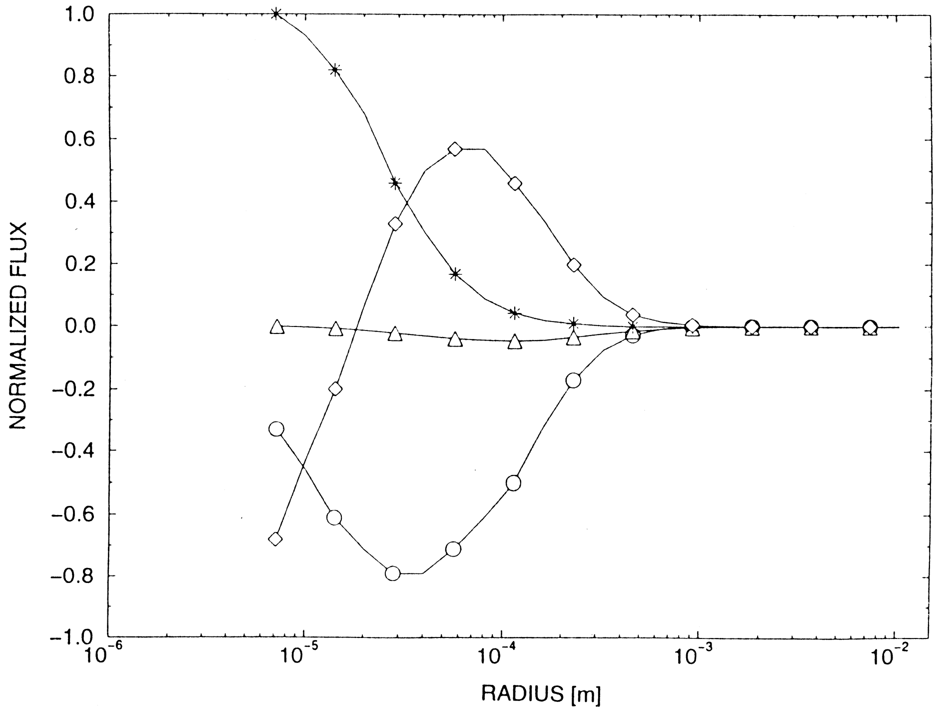
1.0
0.8
0.6
0.4
0.2
0.0
−0.2
−0.4
−0.6
−0.8
−1.0
NORMALIZED FLUX
10^{-6}
10^{-5}
10^{-4}
10^{-3}
10^{-2}
RADIUS [m]

and the mean diameter of suspended crystals. These parameters are found to be only weekly dependent on the surface heat flux and therefore shown as a function of wind only.

The total number of ice crystals is often cited to be around $10^6/\mathrm{m}^3$. For a surface cooling of 200 $\mathrm{W/m}^2$ and a wind of 10 m/s we find from Fig. 2 that the total number of crystals in the boundary layer is predicted to be about 10^9. From Fig. 3, the penetration depth is about 10 m, which gives 10^8 ice crystals/m^3. A closer examination of the results shows, however, that most of the crystals are smaller than 10^{-4} m and may be hard to detect when the number of crystals per m^3 is estimated in an experiment. In fact, if ice crystals with a radius smaller than 10^{-4} m are not considered, the number density is predicted to about 10^7 ice crystals/m^3, which is in fair agreement with earlier estimates.

4.2. Vertical distributions

The vertical distributions of frazil ice volume, number of crystals and mean diameter are found in Fig. 4. These distributions are predicted for a windspeed of 10 m/s and a surface cooling rate of 200 $\mathrm{W/m}^2$. The volume fraction close to the surface is found to be around 10^{-4}, but already at 10 m depth it has decreased with more than an order of magnitude. The number of crystals per unit volume has decreased with an order of magnitude at a depth of 15 m. The mean diameter, as based on the volume and number of particles at a certain depth, is found to decrease down to 10 m and be constant below this depth. Small ice crystals are thus mixed into deeper layers, while the larger ones are found in the upper part of the ocean surface layer.

4.3. Resolution in radial space

When discussing resolution in radial space, the relevant way to specify volumes and numbers is per unit volume and unit radius interval. It is then straightforward to calculate, for example, the number, N, of crystals in the radius interval, $\mathrm{d}r$ and $n\,\mathrm{d}r$, where n is the number per unit radius.

In Fig. 5, the number and volume of three crystal sizes are shown as a function of depth. As seen, the smallest crystals will increase in volume and number from the surface down to about 5 m. The explanation for this behaviour is that the top 10 m are supercooled, and this is thus the region of intense growth. As crystals growth can be viewed as a flux in radial space, this flux gives a sink for the smallest radius shown in Fig. 5.

The distributions in radial space at three selected depths are shown in Fig. 6. The typical slope in these distributions resulted from the calibration of the flocculation process (see Svensson and Omstedt, 1994), and is hence a characteristic feature of the model. The increase at the largest radius interval is not physically correct but an effect of the discretization in the model. Growth and flocculation give a transport in radial space up to the largest radius interval considered. No ice is, however, allowed to leave this interval due to growth or flocculation. An artificial build up of ice is therefore found at the largest radius interval considered. As the build-up is fairly small it is not expected that it affects the main results of the study.

4.4. Balance of process

Next we will consider how the various terms in the crystal number continuity equation balance in the quasi-steady situation studied. As we are interested in the relative importance of the processes, we choose to normalize the processes to fit a diagram with ± 1.0 as bounds.

Vertical distributions of various terms can be found in Fig. 7. Starting with the smallest crystals we find that gravitational effects are insignificant and flocculation is always a sink term. Close to the surface transport by turbulent diffusion balances the net loss due to growth. For the largest crystals gravity causes a sink term while flocculation is a contributing process. Turbulent diffusion always redistributes and is hence bound to be a source in some parts and a sink in others.

Fig. 8 shows the balance in radial space, at two selected depths. The main balance is between growth and flocculation. Of the two processes working in the vertical direction, gravity and diffusion, it is found that diffusion is the more important one. This is, however, somewhat fictitious as it is dependent on the way we choose to represent the fluxes. In Fig. 8, the unit is [Number/m^3, s], which is the same as in the number continuity equation. However, we could also choose the look at the fluxes as [m^3/m^3, s], which implies that we multiply with the unit volume of the crystals at a certain radius. This representation would give large fluxes for the larger crystals and gravity would then be more prominent in the balance. However, as we are interested in the frazil ice regime it is the radius interval 10^{-5} to 10^{-3} m, according to Daly (1994), which ought to be in focus; above the radius 10^{-3} we find the frazil flocs regime.

5. Concluding remarks

The paper presents a first attempt to simulate frazil ice dynamics in the upper layers of the ocean, with resolution in space (with depth), time and radial space. The model formulation includes the main physical processes currently believed to be important, although many of the processes are modelled in the simplest possible way. Basic verification studies of the model, using laboratory measurements, have been presented in the paper of Svensson and Omstedt (1994). Field data, suitable for verification studies, are however still not available, although the recent study by Pegau et al. (1996) shows that instruments for field measurements of frazil ice concentration are available. When such data are available, it will be an interesting task to compare these with the outcome of the model presented. Model results that can be compared with field data include: (1) The suspended ice volume is of the order 5×10^{-4} m^3/m^2; (2) The number of suspended ice crystals is of the order 10^9, for the whole boundary layer. The density of crystals with a radius larger than 10^{-4} m is about $10^7/m^3$; (3) The mean diameter of the ice crystals is about 2×10^{-4} m and decreases with increasing wind speed; (4) The frazil ice concentration decreases rapidly with depth. For a wind speed of 10 m/s and a surface cooling of 200 W/m^2 the concentration [m^3/m^3] decreases with more than one order of magnitude from the surface to a depth of 10 m.

The idealized calculations of frazil ice formation in the upper layers of the ocean indicate that a large number of crystals is mixed into the ocean during freezing. However, the amount of ice in suspension is small as counted as vertically integrated ice thickness. Small crystals are mixed deep while the large ones are found only in the top of the mixed layer. Knowledge about the vertical distribution of ice crystals of different sizes, a major outcome from the model, is believed to be of interest when analysing for example formation of an ice cover in the ocean and ice-sediment or ice-algae interaction.

Acknowledgements

This work has been financed by the Swedish Meteorological and Hydrological Institute and the Swedish Natural Science Research Council under contract G-GU 09151-308.

References

Aagard, K., Coachman, L.K., Carmack, E.C., 1981. On the halocline of the Arctic Ocean. Deep Sea Research A 28, 529–545.

Ackley, S.F., Sullivan, C.W., 1994. Physical controls on the development and characteristics of Antarctic sea ice biological communities: a review and synthesis. Deep Sea Research 41 (10), 1583–1604.

Bauer, J., Martin, S., 1983. A model of grease ice growth in small leads. J. Geophys. Res. 88, 2917–2925.

Bombosch, A., Jenkins, A., 1995. Modeling the formation and deposition of frazil ice beneath Filcher-Ronne ice shelf. J. Geophys. Res. 100 (C4), 6983–6992.

Daly, S. (Ed.), 1994. International Association for Hydraulic Research Working Group on the Thermal Regimes: Report on Frazil Ice. CRREL Special Report 94-23. US Army Cold Regions Research and Engineering Laboratory. Hanover, New Hampshire, USA.

Gow, A.J., Ackley, S.F., Weeks, W.F., Govoni, J.W., 1982. Physical and structural characteristics of Antarctic sea ice. Ann. Glaciol. 3, 113–117.

Hibler, W.D. III, 1979. A dynamic thermodynamic sea ice model. J. Phys. Oceanogr. 9, 815–846.

Jenkins, A., Bombosch, A., 1995. Modeling the effects of frazil ice crystals on the dynamics and thermodynamics of ice shelf water plumes. J. Geophys. Res. 100 (C4), 6967–6981.

Kempema, E.W., Reimnitz, E., Barnes, P., 1988. Sea ice sediment entrainment and rafting in the Arctic. J. Sedimentary Petrology 59 (2), 308–317.

Lange, M.A., 1990. Development and physical properties of sea ice in the Weddell Sea, Antarctica, 22–28. In: Ackley, S.F., Weeks, W.F. (Eds.), Sea Ice Properties and Processes. CRREL Monography 90-1, 300 pp.

Leppäranta, M., 1983. A growth model for black ice, snow ice and snow thickness in subarctic basins. Nordic Hydrology, 59–70.

Leppäranta, M., 1993. A review of analytical models of sea ice growth. Atmosphere–Ocean 31 (1), 123–138.

Martin, S., 1981. Frazil ice in rivers and oceans. Ann. Rev. Fluid Mech. 13, 379–397.

Martin, S., Cavalieri, D.J., 1989. Contributions of the Siberian shelf polynyas to the Arctic Ocean intermediate and deep water. J. Geophys. Res. 94 (C9), 12725–12738.

Maykut, G.A., 1986. The surface heat and mass balance. In: Untersteiner, N. (Ed.), The Geophysivs of Sea Ice. The NATO ASI Series, B 146. Plenum Press, USA, 395–463.

Maykut, G.A., Untersteiner, N., 1971. Some results from a time-dependent, thermodynamic model of sea ice. J. Geophys. Res. 76 (6), 1550–1575.

Nurnberg, D., Wollenburg, I., Dethleff, D., Eicken, H., Kassens, H., Letzig, T., Reimnitz, E., Thiede, J., 1994. Sediments in the Arctic sea ice: implications for entrainment, transport and release. Marine Geology, 119.

Omstedt, A., 1985a. On supercooling and ice formation in turbulent sea water. J. Glaciol. 31 (109), 263–271.

Omstedt, A., 1985b. Modelling frazil ice and grease ice formation in the upper layers of the ocean. Cold Region Science and Technology 11, 87–98.

Omstedt, A., Svensson, U., 1984. Modelling supercooling and ice formation in a turbulent Ekman layer. J. Geophys. Res. 89 (C1), 735–744.

Omstedt, A., Sahlberg, J., Svensson, U., 1983. Measured and numerically simulated autumn cooling in the Bay of Bothnia. Tellus 35 A, 231–240.

Pease, C.H., 1987. The size of wind-driven coastal polynyas. J. Geophys. Res. 92, 7049–7059.

Pegau, W.S., Paulson, C.A., Zanevald, J.R.V., 1996. Optical measurements of frazil concentration. Cold Regions Science and Technology 24, 341–353.

Pfirman, S., Lange, M.A., Wollenburg, I., Schlosser, P., 1990. Sea ice characteristics and the role of sediment inclusions in deep sea deposition. Arctic and Antarctic comparisons. In: Bleil, U., Thiede, J. (Eds.), Geological History of the Polar Oceans: Arctic versus Antarctic, 187–211. Kluwer Academic Publishers, The Netherlands.

Reimnitz, E., Kempema, E.W., 1987. Field observations of slush ice generated during freeze-up in Arctic coastal waters. Marine Geology 77, 219–231.

Rodi, W., 1980. Turbulence models and their application in hydraulics—a state of the art review. Int. Assoc. Hydr. Res., Section Fundam. Div. 2: Exp. Math. Fluid Dyn., Delft, The Netherlands.

Rodi, W., 1987. Examples of calculation methods for flow and mixing in stratified flows. J. Geophys. Res. 92, 5305–5328.

Smith, S.D., Muench, R.D., Pease, C.H., 1990. Polynyas and leads: an overview of physical processes and environment. J. Geophys. Res. 95 (C6), 9461–9479.

Stefan, J., 1891. Uber die Theorie der Eisbildung, insbesondere uber Eisbildung im Polar Meeres. Ann. Physik 42, 269–286, 3rd Ser.

Svensson, U., 1986. PROBE—An Instruction Manual. SMHI Reports Oceanography, 10, SMHI, S-601 76 Norrrköping, Sweden, 90 pp.

Svensson, U., Omstedt, A., 1994. Simulation of supercooling and size distribution in frazil ice dynamics. Cold Regions Science and Technology 22, 221–233.

Ushio, S., Wakatsuchi, M., 1993. A laboratory study on supercooling and frazil ice production processes in winter coastal polynyas. J. Geophys. Res. 98 (C11), 20321–20328.

Wadhams, P., Lange, M.L., Ackley, S.F., 1987. The ice thickness distribution across the atlantic section of the Antarctic Ocean in midwinter. J. Geophys. Res. 92 (C13), 14535–14552.

Wadhams, P., Comiso, J.C., Prussen, E., Wells, S., Brandon, M., Aldworth, E., Viehoff, T., Allegrino, R., Crane, D.R., 1996. The development of the Odden ice tongue in the Greenland Sea during winter 1993 from remote sensing and field observations. J. Geophys. Res. 101 (C8), 18213–18235.